Semiannual Technical Summary

Distributed Sensor Networks

DTIC
ELECTE
FEB 10 1986
S   D
B

30 September 1985

Lincoln Laboratory

MASSACHUSETTS INSTITUTE OF TECHNOLOGY

LEXINGTON, MASSACHUSETTS

This technical report has been reviewed and is approved for publication.

FOR THE COMMANDER

Thomas J. Alpert, Major, USAF
Chief, ESD Lincoln Laboratory Project Office

MASSACHUSETTS INSTITUTE OF TECHNOLOGY
LINCOLN LABORATORY

DISTRIBUTED SENSOR NETWORKS

SEMIANNUAL TECHNICAL SUMMARY REPORT
TO THE
DEFENSE ADVANCED RESEARCH PROJECTS AGENCY

1 APRIL — 30 SEPTEMBER 1985

ISSUED 8 JANUARY 1986

DTIC
S ELECTE **D**
FEB 10 1986
B

"Original contains color
plates: All DTIC reproduct-
ions will be in black and
white"

LEXINGTON   MASSACHUSETTS

ABSTRACT

This report describes the work performed on the DARPA
Distributed Sensor Networks Program at Lincoln Laboratory
during the period 1 April through 30 September 1985.

Accession For		
NTIS GRA&I	✔	
DTIC TAB	☐	
Unannounced	☐	
Justification		
By		
Distribution/		
Availability Codes		
Dist	Avail and/or Special	
A-1		

QUALITY INSPECTED 3

iii

TABLE OF CONTENTS

LIST OF ILLUSTRATIONS

DISTRIBUTED SENSOR NETWORKS

I. INTRODUCTION AND SUMMARY

The Distributed Sensor Networks (DSN) Program is aimed at developing and extending target surveillance and tracking technology in systems that employ multiple spatially distributed sensors and processing resources. Such a system would be made up of sensors, data bases, and processors distributed throughout an area and interconnected by an appropriate digital data communication system. The detection, tracking, and classification of low-flying aircraft have been selected to develop and evaluate DSN concepts in the light of a specific system problem. A DSN test bed has been developed and is being used to test and demonstrate DSN techniques and technology. The overall concept calls for a mix of sensor types. The initial test-bed sensors are small arrays of microphones at each node augmented by TV sensors at some nodes. This Semiannual Technical Summary (SATS) reports results for the period 1 April through 30 September 1985.

Test-bed and tracking system improvements are described in Section II. These include the completion of a TV subsystem that has been added to the test bed, changes in tracking software to integrate and utilize the TV subsystem, the automation of test-bed interactions to improve usability, and the addition of floppy disks to test-bed nodes for data logging and for providing an additional data source for experiments.

Section III describes a series of real-time test-bed demonstrations that were performed during this reporting period. A six-node demonstration of distributed acoustic tracking and robust system behavior was presented during the DSN contractors workshop hosted by Lincoln Laboratory. This involved real-time tracking with simulated helicopter data read from tapes mounted on the test-bed signal-processing systems. Real-time tracking, target handover, and robust system behavior when faced with a communication failure were demonstrated as was the simultaneous use of two user workstations with color displays to show tracking results. Real-time acoustic and TV tracking were also demonstrated at the workshop. Data from the acoustic array of one of the test-bed nodes were used to perform real-time tracking of a UH-1 helicopter. The TV subsystem was linked to the tracking system and also was used to perform real-time tracking of the same helicopter. This demonstrated the real-time signal-processing and measurement capabilities of the acoustic and TV subsystems in the test bed. Another demonstration was performed internally to validate the nodal data logging and reading capabilities, and to provide data for multisite integration efforts. That demonstration used a total of eight test-bed nodes to track two simulated helicopters and to log the tracking results on the floppy disks.

In Section IV, we reports the results of three different acoustic tracking evaluation efforts.

First, a series of experiments was carried out to investigate the trade-offs between tracking performance and communication policies. These experiments used prerecorded data collected by four DSN nodes. The target was a nonmaneuvering UH-1 helicopter. A minimal communication

Keywords: acoustic arrays; digital radios.

policy was shown to provide satisfactory tracks by the time the helicopter reached the fourth node in the system. The primary advantage of additional communications was to decrease the size and duration of the initial transient errors in the track.

Second, a series of two-node experiments was run to test the sensitivity of the tracker to target velocity and maneuvers. Simulated acoustic measurements were generated for two nodes separated by 5 km and a number of test cases. Two test-bed nodes were used to apply the tracker to the simulated data sets at a real-time rate. Tracker parameters previously selected for the low-speed helicopter experiments were used for these experiments. Track initiation occurred further along the track for high-speed targets compared with low-speed targets, and tracking errors were generally smaller for the low-speed targets for which the tracking parameters were adjusted. The two-node tracker recovered reasonably well from a 45° dog-leg maneuver between the nodes by a Mach 0.1 target, and somewhat less well from a speed change from Mach 0.1 to 0.2. For both maneuvers, part of the difficulty was that, with only two nodes, there was insufficient downstream information about the maneuver.

Third, an acoustic data collection experiment was completed using an aircraft instrumented to provide ground truth. This was primarily intended to shake down procedures for using ground-truth information recorded on the aircraft in preparation for more extensive future experiments with a different but similarly instrumented aircraft.

Section V reports on the development of a DSN signal-processing diagnosis system to demonstrate the feasibility of applying current Artificial Intelligence technology to such a problem.

II. DISTRIBUTED TRACKING SYSTEM IMPROVEMENTS

During this reporting period, substantial improvements to the DSN test-bed software and tracking system were completed. They fall into three major classes: development of a TV subsystem, enhancements to test-bed tracking nodes, and improved tools for test-bed users.

A TV subsystem is being developed to demonstrate tracking improvements resulting from the cooperative use of sensors with complementary properties, and to investigate the management of the interaction between these sensors. The TV node accepts position messages from a tracking node. These messages consist of a time tag and position tracks (estimated state vector and error covariance matrix) for one or more targets. The TV subsystem produces as output an azimuth message which is sent back to the tracking node. The output message consists of a time tag and an azimuth measurement for one of the tracks in the input message.

The TV subsystem processing is organized into the three functions shown in Figure II-1. First, the algorithm selects one target (one track) and determines how the camera should be moved to point at this target. Next, two sequential image frames are taken and their difference is formed to produce an image emphasizing the outlines of moving objects within the field of view. Finally, the location of the target within the difference image is estimated and the corresponding azimuth is computed.
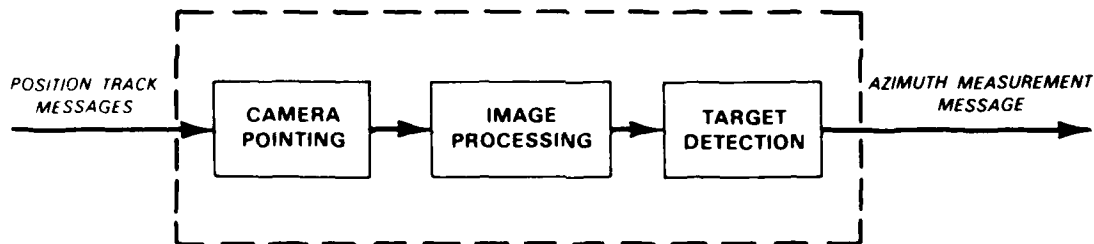
Figure II-1. TV node algorithm elements.

The camera pointing algorithm is organized into the two stages shown in Figure II-2. First, four "features" are computed for each of the tracks in the position message and both slew directions (clockwise and counterclockwise). The features are: (1) the first time at which the camera can acquire the target as it slews in the specified direction, (2) the length of the time interval during which the target can remain in the camera field of view after acquisition, (3) the range from the camera to the target at the predicted acquisition time, and (4) the target azimuth at the predicted acquisition time. Second, based on the computed features, the algorithm selects a target and camera slew direction and controls the camera to point at the selected target. The pointing algorithm that has been implemented and used for initial experimentation selects a target based upon a minimum acquisition time criterion. A more intelligent pointing algorithm that will make use of all the features is under development.

3

```
POSITION TRACK
   MESSAGE          ┌──────────────┐                  ┌──────────┐      CAMERA SLEW
                    │   FEATURE    │                  │ DECISION │       COMMAND
  ─────────────────▶│  EXTRACTION  │─────────────────▶│   RULE   │─────────────────▶
                    │              │    FEATURES      │          │
                    └──────────────┘                  └──────────┘
```
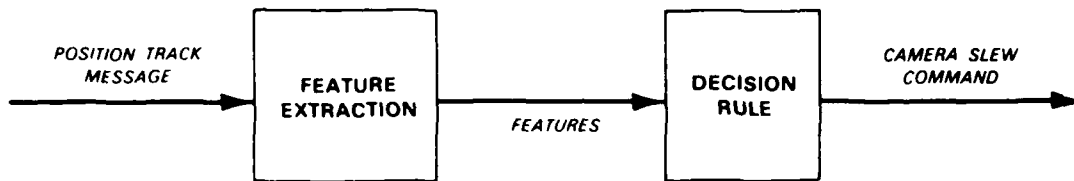
157909-N

Figure II-2.   Camera pointing algorithm.

The objectives of the TV subsystem development effort during this report period included developing software to interface the video node with other DSN nodes and upgrading hardware components to enhance system performance. Progress was made in each of these two areas as follows.

Previously developed image-processing and target-detection algorithms were refined, and all elements were integrated to form a complete TV subsystem. Integration required software modules to synchronize the TV subsystem clock with the tracking system clock, to receive and interpret ethernet messages from the tracker, and to construct and send ethernet messages to the tracker.

Hardware changes also were made to the camera mount in the TV subsystem. A heavy-duty mount was installed to provide more precise pointing, more accuracy in measuring the camera direction, and to increase the azimuth slewing speed. Modifications were made to the mount readout electronics to achieve these goals. A single-speed synchro, coupled to the azimuth shaft through anti-backlash gears, was installed to allow the computer to read the camera pointing direction to within plus or minus one-tenth of a degree. A second mount was also purchased and is presently undergoing the modifications for use in a second TV subsystem. Software changes to make use of the improved mount capabilities have been implemented but not yet fully tested.

The most significant tracking-node improvements relate to the integration of the TV subsystem with the tracking software. Any tracking node can now provide cueing information to a TV subsystem. The tracking node delivers all its tracks to the TV subsystem, which is responsible for selecting the specific targets upon which the TV subsystem will concentrate. Software switches control which node cues the TV subsystem. Additions were also made to the tracking software to use azimuth measurements reported by the TV subsystem. Because the tracking algorithm is general and its implementation modular, this required only the addition of a small number of new subroutines specifically designed to update target tracks with TV azimuth measurements.

Changes were made to nodal system software in the Standard Nodal Computers (SNCs) to allow application software to read and write files on the floppy-disk systems attached to each node. This was required to support two tracking software enhancements which greatly increase the usability of the test bed.

Before the floppy-disk capabilities were added to the SNC system, acoustic azimuth measurements could be obtained only through the hardware interface between the SNC and an

4

attached Sound Processing Subsystem (SPS), which is used for data collection and real-time signal processing. Now, azimuth measurement data (either simulated or preprocessed), can be recorded on a floppy disk and read by the tracking software as if it came from the SPS/SNC interface. This allows experiments to be performed using nodes which do not have an SPS or on which the SPS is not operational. There are now three nodes without as well as six nodes with SPSs, giving us a nine-node test bed when all the mobile nodes are available and a six-node test bed when the mobile nodes are in the field.

The floppy-disk system now can also be used to record tracking performance data for subsequent analysis. In the past, these data were transmitted over the test-bed ethernet to a VAX-11 780 for recording. Some of this information was lost due to the need to keep up with real time, especially when many nodes were used or a large of amount of detailed information was required. This situation was particularly unsatisfactory for real-time experiments which are impossible to repeat in detail. Experimenters can now record data on the floppy disks without loss of data, and can modify software to record more detailed internal operations of the tracking algorithm. The floppy-disk recordings produced by the nodes can be read on the VAX-11/780 for post-experiment analysis.

Additional work with the Nodal Run-Time System (NRTS) was directed at integrating Communication Network Technology radios into the DSN test bed. Radio broadcast software has been integrated with NRTS and tested in loop-back mode with a single radio interface unit. Further tests are planned with back-to-back interfaces before final testing with radios. As part of this activity, additional documentation of the NRTS was written.

Modifications of ethernet communications software and the User Interface Program (UIP) that provides the user interface to the test bed were completed to permit experiments to be controlled from the two Silicon Graphics, Inc. (SGI) workstations as well as from the VAX-11/780. This change will allow future Air Vehicle Survivability Evaluation project field experiments to be controlled via a workstation. The SGI systems also allowed the use of color displays and facilitated the switching between the various graphical displays available to the user. As a result, it is now much easier for experimenters to understand what is occurring during real-time experiments.

While experimenters use the UIP and the ethernet for most of the interactions with the test bed, they must also communicate via serial lines with a primitive monitor system in each node in order to load and start the software which communicates with the UIP. This communication need not be done every time a new experiment is run, but is necessary whenever the experimenter runs a different version of the tracking software or whenever a node has been powered down. The elementary interactions with the monitor system are cryptic, and even experienced experimenters are apt to make errors. To minimize errors, reduce training time for new experimenters, and generally facilitate the use of the test bed, the most common interactions were automated during this reporting period.

In addition, test-bed diagnostic programs have been written to help determine which parts of which nodes are operational when there is a problem.

Blank Page

III. REAL-TIME TEST-BED DEMONSTRATIONS

A. ROBUST SIX-NODE OPERATION

A six-node demonstration of distributed acoustic tracking and robust system behavior was given as part of the DSN workshop hosted by Lincoln Laboratory in June. The demonstration used synthetic acoustic measurement data played back over the SPS/SNC interfaces in real time.

Figure III-1 shows the geometric layout of the nodes relative to each other and to the flight paths of two simulated helicopters. The nodes were 5 km apart in a rectangular pattern, with the helicopters flying down the length of the rectangle at a simulated velocity of Mach 0.1. The flight paths were separated by a kilometer laterally, with the upper helicopter's path centered in the rectangle and with the lower helicopter delayed by 50 s relative to the upper. The detection threshold in each node was set to give a maximum detection range of 5 km and the nodes communicated as if their radio range was limited to 5 km.
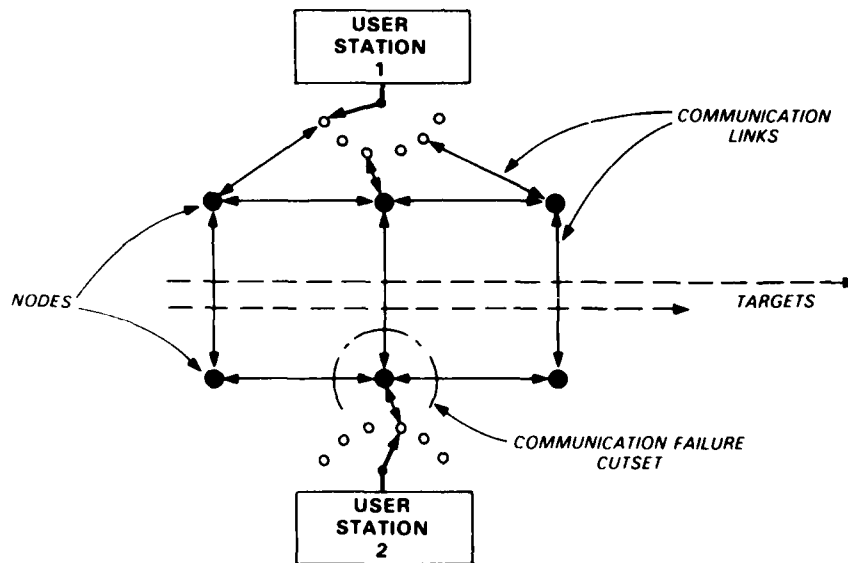
Figure III-1. Robust multinode tracking demonstration.

The figure also indicates the two SGI user workstations that were employed simultaneously to collect and display experimental results. Station 1 was used to examine data from all the nodes. Station 2 was used to examine internal data from a single node, which was isolated from the rest of the network by a simulated communication failure during part of the experiment to demonstrate robust system operation.

7

Figure III-2 reproduces one of the SGI color displays which appeared in the demonstration. Triangles indicate the locations of the first four nodes encountered. The display shows all the position tracks broadcast by the lower-left node at the completion of the demonstration. The actual display evolved in real-time during the experiment. The track for the lower helicopter did not appear until the upper one was almost beyond range of the first two nodes. The real-time display was updated every 2 s. A blue "*" was plotted at the current true location of each helicopter, and a yellow "O" at the position estimated by the tracker. The true location could be shown since simulated data were used in the experiment. The red ellipse surrounding each estimated position represented the uncertainty assigned to the location estimate by the tracker.

The initial location estimate for the upper target appears about 3 km from either node in spite of the fact that the nodes have a 5-km detection range. This is due to two kinds of delay: algorithm and acoustic propagation. The algorithm delay results because position track initiation requires the use of two well-established azimuth tracks and this requires several 2-s observation cycles. Acoustic-propagation delays cause the target to be closer than its acoustic detection range when we first hear it. For example, the helicopter is 4.5 km from the nodes when the sound emitted at a range of 5 km is received. The acoustic-delay effect appears even more obvious for the lower target because it is further away from the upper node for this case.

In both cases, the uncertainty in the location estimates initially decreases, then increases slightly as the targets pass between the first two nodes, and shortly thereafter decreases substantially. The initial decrease is due to additional azimuth measurements and a good geometrical configuration. The increase, when the targets pass between the first two nodes, is because azimuth measurements provide no location information along the line joining the two nodes. The sudden large decrease in errors occurs when the targets come within range of the next nodes and their azimuth measurements are integrated into the position tracks.

This experiment demonstrated the robustness of the tracking algorithm by simulating a communications failure for the lower-middle node just before that node was alerted to the presence and track of the second helicopter by its neighbors. Communications were restored shortly after the second helicopter passed between the two middle nodes. Figure III-3 shows the tracks created by the upper-middle node, and Figure III-4 shows those created by the lower-middle node. Note the long period during which the upper node tracks the second helicopter but the lower node does not. The lower node cannot initiate track without help from another node. Once communications are restored, it obtains information to initiate track and begins tracking as accurately as the upper-middle node.

B. LIVE ACOUSTIC AND TV TRACKING

A real-time acoustic and TV tracking experiment with a live UH-1 helicopter target was performed during the DSN workshop in June. This demonstrated real-time acoustic signal processing and TV image processing as well as target tracking. For this demonstration, both the acoustic and TV tracking were manually cued.

8

Figure III-2. Final track display for lower-left mode of tracking demonstration shown in Figure III-1
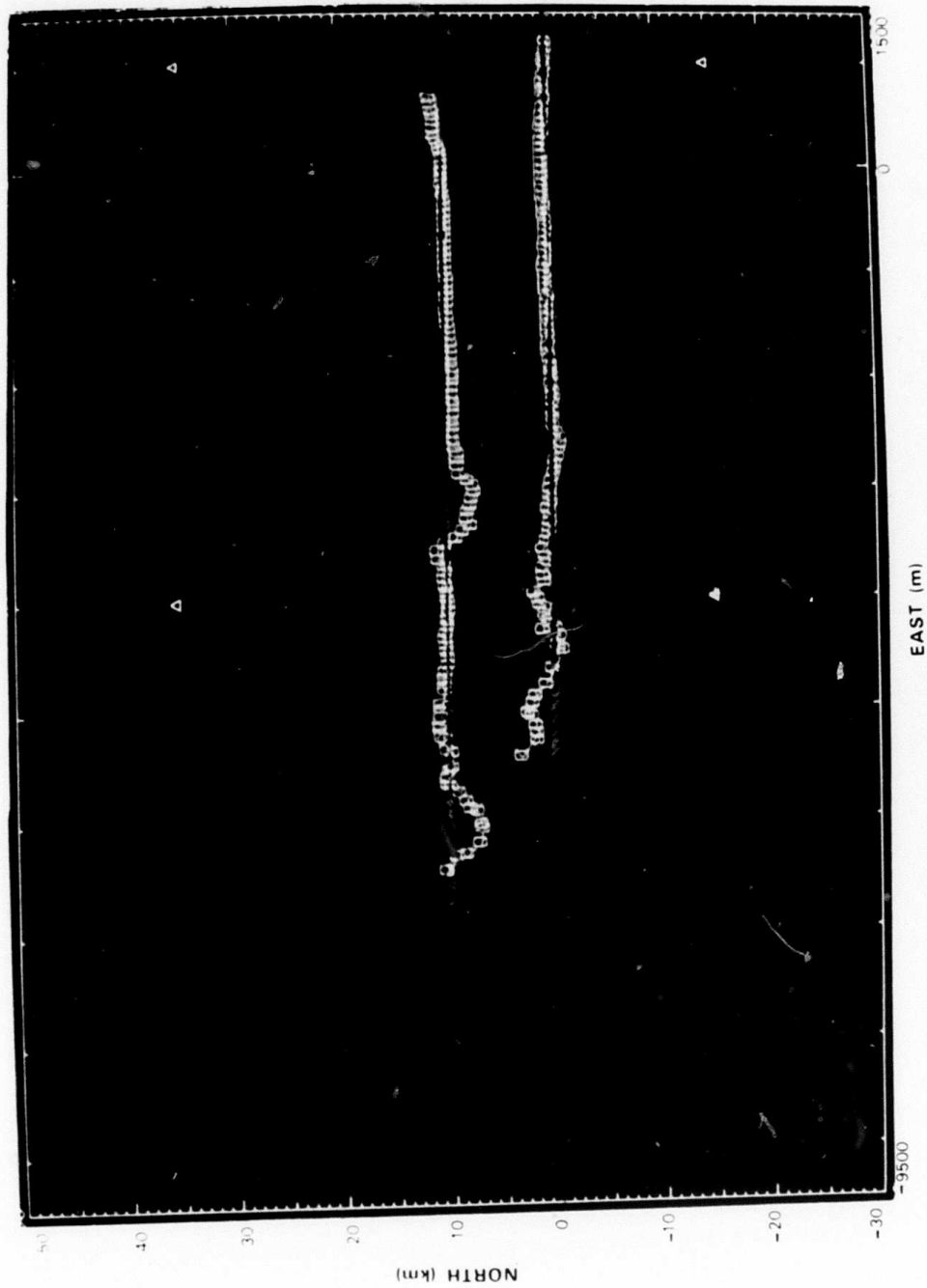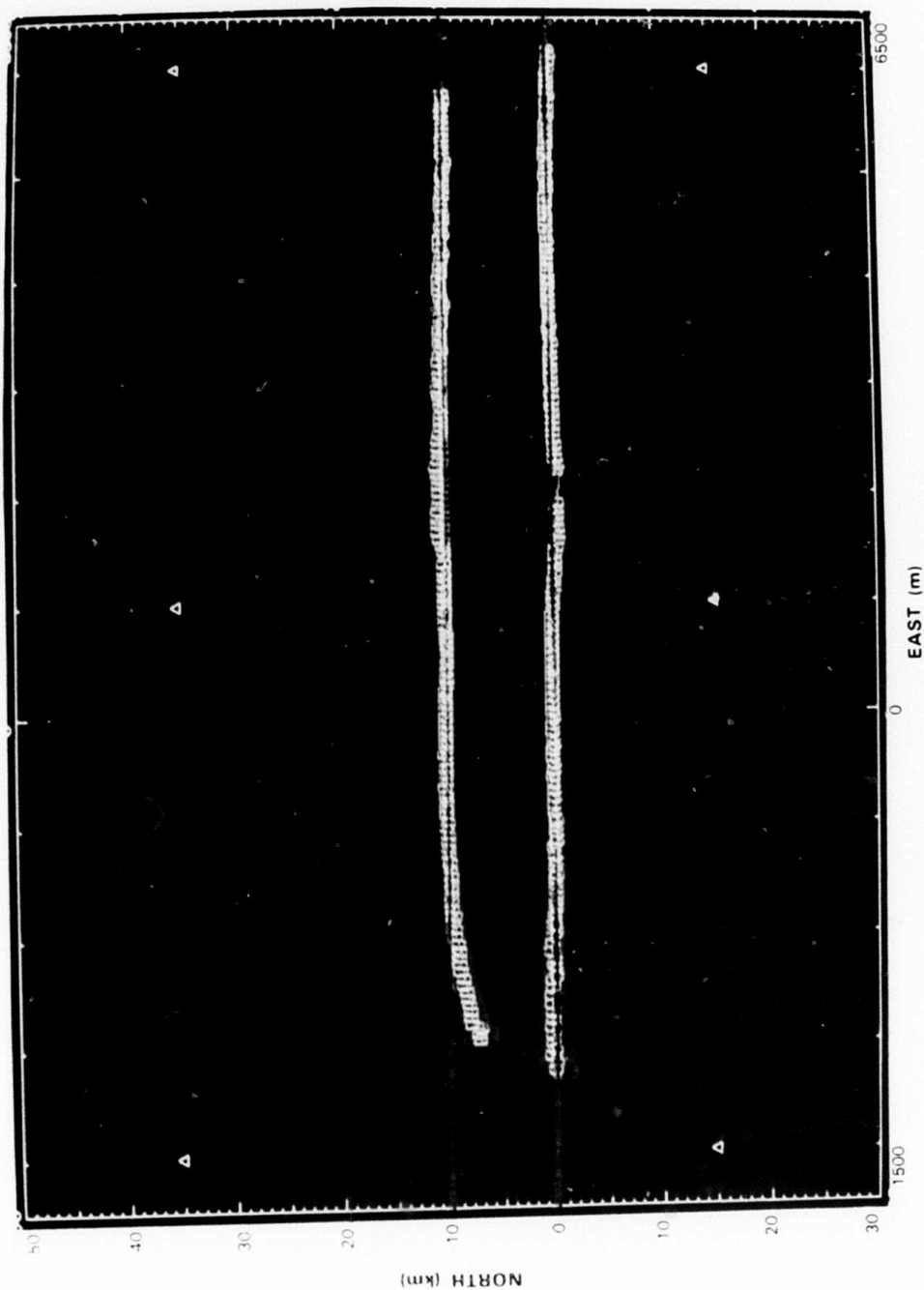
EAST (m)

NORTH (km)

157985 N

9

Figure III-3. Final track display for upper-middle node of tracking demonstration shown in Figure III-1.
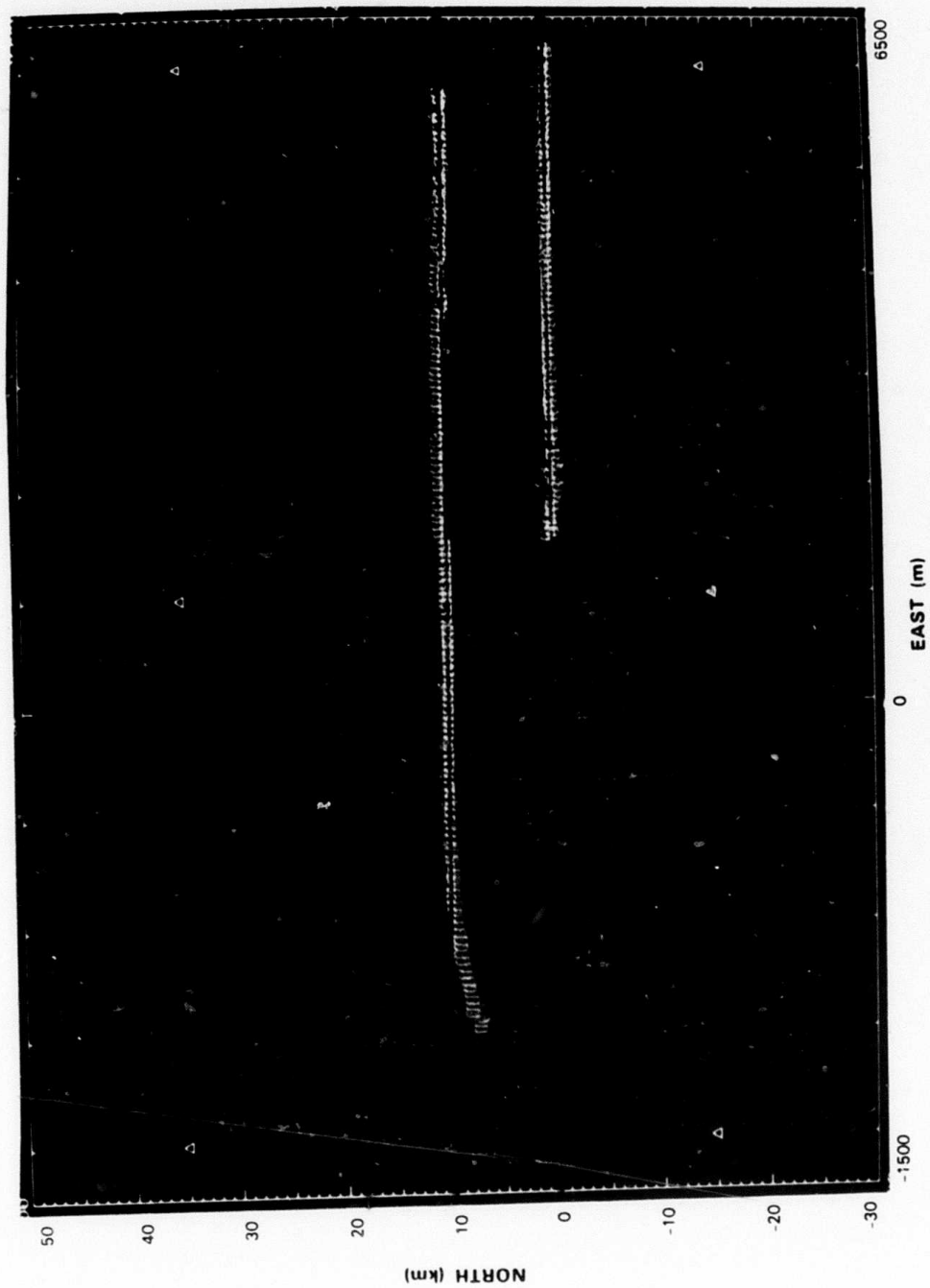
157993 N

Figure III-4. Final track display for lower-middle node of tracking demonstration shown in Figure III-1. Simulated temporary communication failure resulted in late start of lower target track.
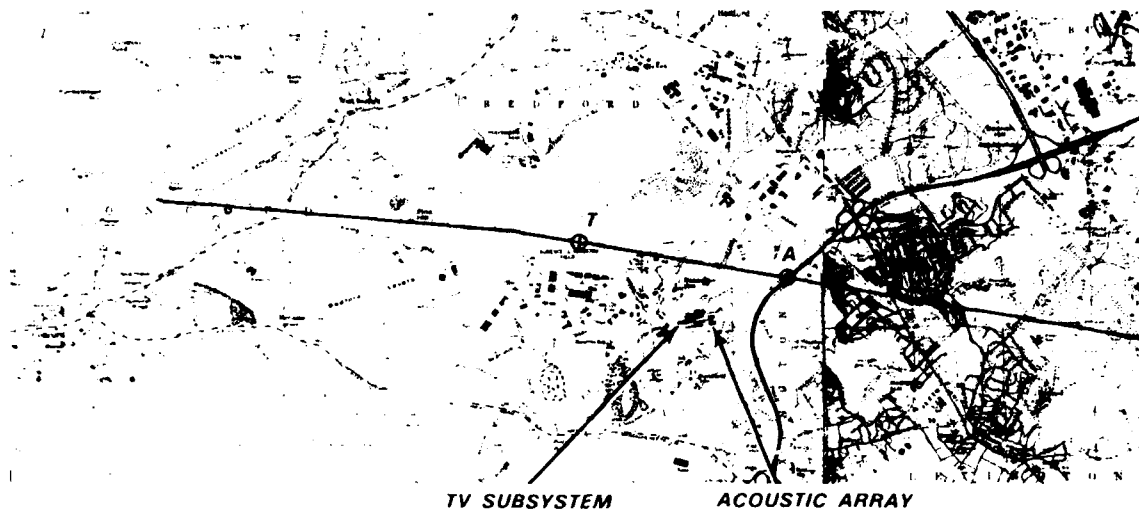
157994-N

13 preceding page not filmed

TV SUBSYSTEM   **ACOUSTIC ARRAY**

Figure III-5   Live tracking demonstration flight path. Points A and T show where the acoustic and TV subsystems, respectively, were manually cued.

A UH-1 helicopter flew a preplanned course during the demonstrations. Figure III-5 illustrates the flight path relative to Lincoln Laboratory. The helicopter flew from right to left (westerly) at roughly Mach 0.1. The locations of the acoustic sensor array and TV camera used in the experiment were at opposite ends of the Laboratory complex as shown on the figure. A checkpoint (A) on the track was selected to begin acoustic tracking, and a second checkpoint (T) was selected to begin TV tracking. An observer in the helicopter called out on a radio link his passage over those landmarks, and tracking was manually initiated.

Figure III-6 shows the overall experiment concept. The two tracking nodes and the alerting node were all standard test-bed SNC nodes. The acoustic subsystem consisted of a set of microphones, A/D equipment, an array processor, and a PDP-11 34 used for control. The TV subsystem consisted of a standard SNC augmented with TV equipment. All message communication was via the test-bed ethernet, except for azimuth messages from the acoustic subsystem which has a direct connection to its associated tracking node. When the target was at checkpoint A, a button was pushed on the alerting node which sent a track initiation message to the acoustic tracking node. The acoustic tracking node then proceeded to track the target using real-time acoustic azimuth measurements provided by the real-time acoustic subsystem. When the target reached checkpoint T, a second alerting message was sent to the TV tracking node which then proceeded to track the target using real-time TV-derived azimuth measurements.

Figure III-7 illustrates the real-time acoustic tracking results. A crude outline of the Lincoln Laboratory, nearby Route 128, and part of the Hanscom runways is included in the figure for reference. The track accuracy improved for a while after track initiation, and then degraded because the azimuth measurements can only decrease position uncertainty in the crossrange direction. The target track was eventually terminated when the uncertainty ellipse became very large in the direction radial to the acoustic array.

15
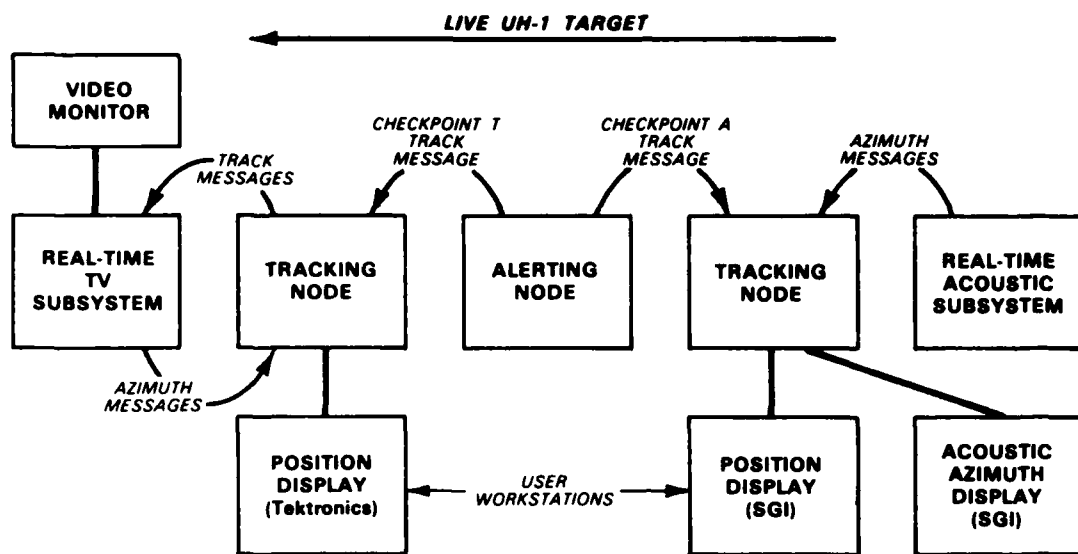
Figure III-6. Live acoustic and TV tracking demonstration concept.
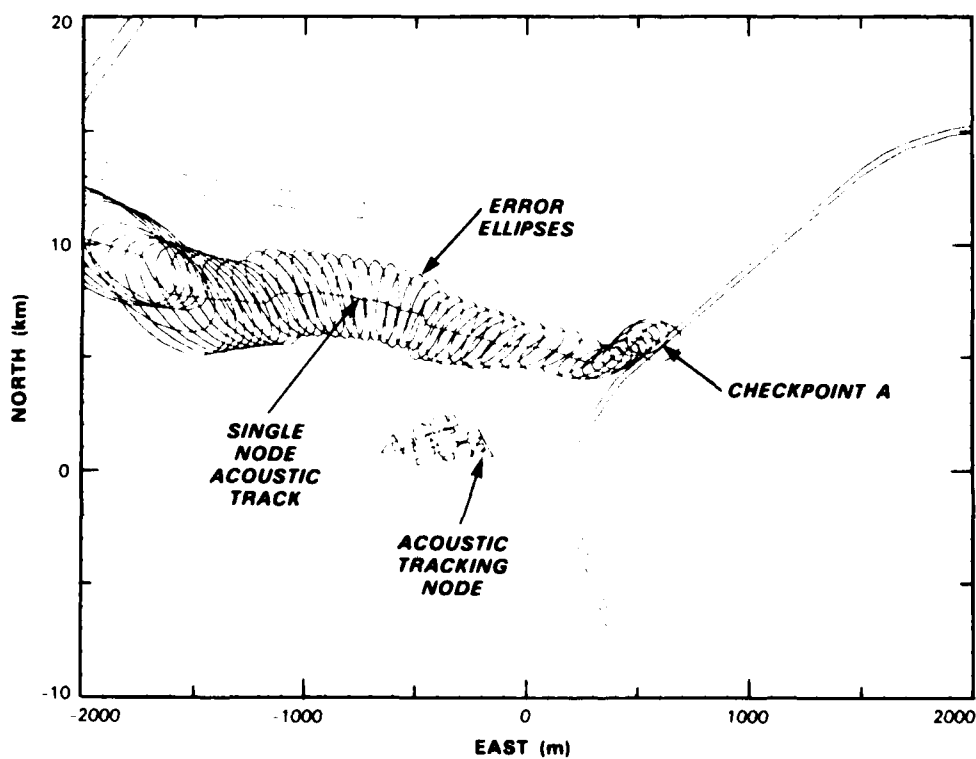
Figure III-7. Live acoustic demonstration helicopter track.

16

The TV tracking results are shown in Figure III-8. The TV subsystem was prepositioned in the correct direction for the first TV azimuth measurement. When the cueing message was received, the TV subsystem proceeded to perform signal processing, extract an azimuth measurement, and return it to the tracker. Subsequently, the TV subsystem and tracker operated as a coordinated closed-loop system with the TV accepting track updates from the tracker, slewing to new target position, and providing a sequence of azimuth measurements that were used by the tracker node to update tracks. The target track and error covariance estimates generated by the tracking node were displayed in real time as the experiment progressed. The TV track was initiated with a circular error ellipse having a radius of 500 m. As video measurements were processed, the error ellipse shrank in the direction perpendicular to the camera line-of-sight, since TV azimuth measurements can only reduce uncertainty in that direction. This is similar to the situation with acoustic azimuth measurements except that, in the case of the TV, measurements have no built-in time delay. Eventually, the TV system ceased making new measurements and the position track coasted, with the error ellipses growing, until the errors became large enough so that the tracking algorithm terminated. This experiment was the first real-time demonstration of how the video system can, upon receipt of the appropriate cue, acquire and track a target and provide a standard DSN tracker with measurements to reduce target location uncertainty.
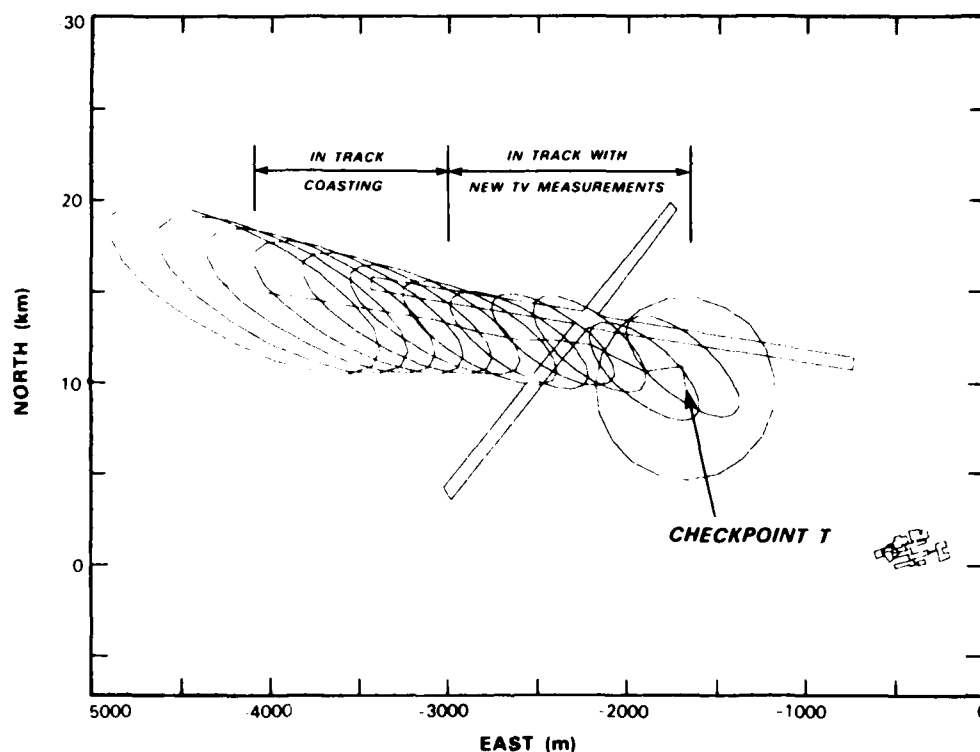

Figure III-8.   Live TV demonstration helicopter track.

157982-N

17

C. EIGHT NODES WITH DATA LOGGING

As described in Section II, a capability was implemented to read simulated data from and log data to floppy disks. Validation tests of this capability were done in which eight test-bed nodes were used. The data were synthetic acoustic azimuths that were read in real time from the nodal floppy disks by the tracking software. This allowed a real-time eight-node experiment to be executed, although only six nodes have complete signal processing subsystems. The synthetic acoustic measurement data were identical to the data used in the robust six-node operation demonstration described in Section III-A, except that two more nodes were included. Figure III-9 shows the layout of all eight nodes and the simulated tracks for the two helicopters.
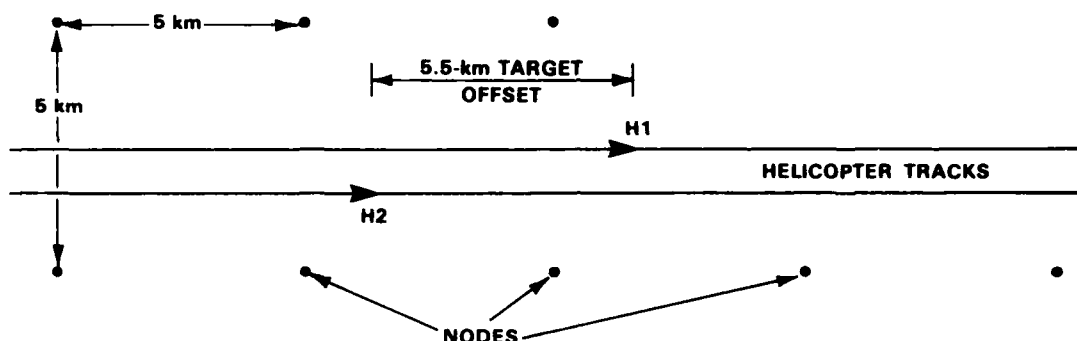

Figure III-9. Node location and helicopter tracks for eight-node experiment with data logging.

In addition to providing a validation of the new test-bed capabilities, the tests have also provided an initial multinode data set, including both local and common tracks, for developing and testing multisite integration capabilities. Previously, only local nodal tracks could be obtained from the test bed and some nodal data were lost due to the limitations of data collection over the test-bed ethernet. The more complete data sets will allow us to develop and test multinode combining algorithms similar to those used in nodal tracking algorithms.

Figure III-10 illustrates the general procedures for running an experiment using the floppy disks. As described in Section II, the Nodal Run-Time System (NRTS) as well as the application software were modified to support these functions. At the start of the experiment, separate input data and logging disks are mounted on each of the test-bed nodes. At the end of the experiment, all the logging floppy disks are removed and transported to a VAX where they are read in for post-experiment analysis. VAX software was developed to read the logging disks into UNIX files and to write the simulated acoustic data to the disks. Several experimental runs can be made with the same physical logging floppy and the results stored on different partitions of the disk. Several sets of input data can also be put on different partitions of the floppy disks for the nodes.
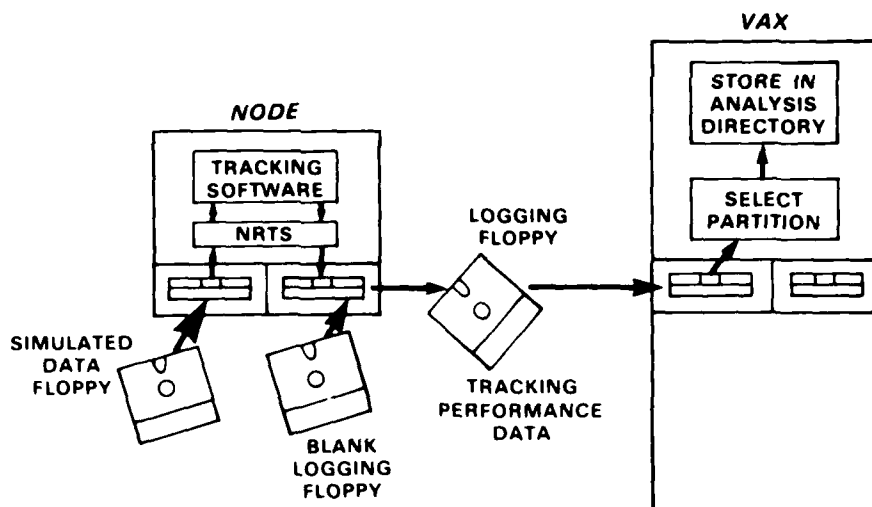
Figure III-10. Operational procedures for the use of nodal disk systems for simulated data input and performance logging.

Nodal operational procedures are the same as for other test-bed modes except for a few parameter modifications and the physical location of the data and results. A special process is enabled to initiate using the floppy disks and to specify whether they are being used for data input, for logging, or for both. The signal processor is notified that the tracking software is configured to read data from the floppy disks rather than from the interface to the signal processing subsystem. In all cases, the tracking software can forward tracking performance data through the ethernet to the user workstation for immediate display, although some data may be lost due to ethernet limitations in a real-time environment. Nevertheless, the nodal disks will contain the entire data set.

19

IV. ACOUSTIC TRACKING EVALUATION

A. COMMUNICATION POLICY EXPERIMENTS

A series of experiments was completed to investigate the interactions between tracking system performance and communication algorithms that decide when to broadcast. The results were presented at the 1985 Joint Automatic Control Conference, at the 1985 MIT/ONR Workshop on Distributed Communication and Decision Problems, and at the DSN Workshop hosted by Lincoln Laboratory in June. The experiments were conducted using real acoustic data recorded by four test-bed nodes. The data were for a UH-1 helicopter flying a straight path at Mach 0.1 in the vicinity of Lincoln Laboratory. The flight path was the same as that of Figure III-5, but with more checkpoints. An observer recorded times at which each checkpoint was passed to provide ground-truth data.

Communication algorithms that implement a range of broadcast policies that depend upon both temporal and spatial conditions have been integrated with the tracking system and were used for these experiments. In all cases, position tracks are broadcast when a track is initiated. A position track is also broadcast by a node when the the target is estimated to have passed out of the coverage area of its own sensor or to have passed into the sensor coverage of another node. The track is dropped by the broadcasting node in a case where the target is believed to be beyond the coverage of its own sensor. Broadcasting when these critical events take place prevents important measurement information about the target from being lost or poorly used. In addition, the algorithm places a limit upon the time interval between broadcasts for each node. When that limit is exceeded, regardless of whether a critical-event occurs or not, a track is broadcast. All rules apply separately to each target.

The communication experiments involved changing the maximum time interval and assumed sensor coverage, and operating with and without the critical-event broadcasts. Most of the results were as expected. Decreasing the maximum interval between broadcasts generally improves tracking performance, but the improvement is largely in reducing the time required to achieve a relatively accurate track. Once a good track has been achieved, the value of extra broadcasts is much less. Critical-event broadcasts are most important when the time limit is large. Otherwise, regular broadcasts tended to occur close enough to the critical events to result in little loss or misuse of information.

The sensor coverage models used by the communication and tracking algorithms are circles centered at each node, with the radius of the circle being the only adjustable parameter. Our experiments showed that this model is at best a crude approximation. For our experiment, the helicopter was detected further away when approaching a node than when receding from it. The magnitude of the difference varied from sensor to sensor, but was never less than two-to-one. It was possible to operate the system with the simple circular model, but a more sophisticated model might make better use of all of the available data.
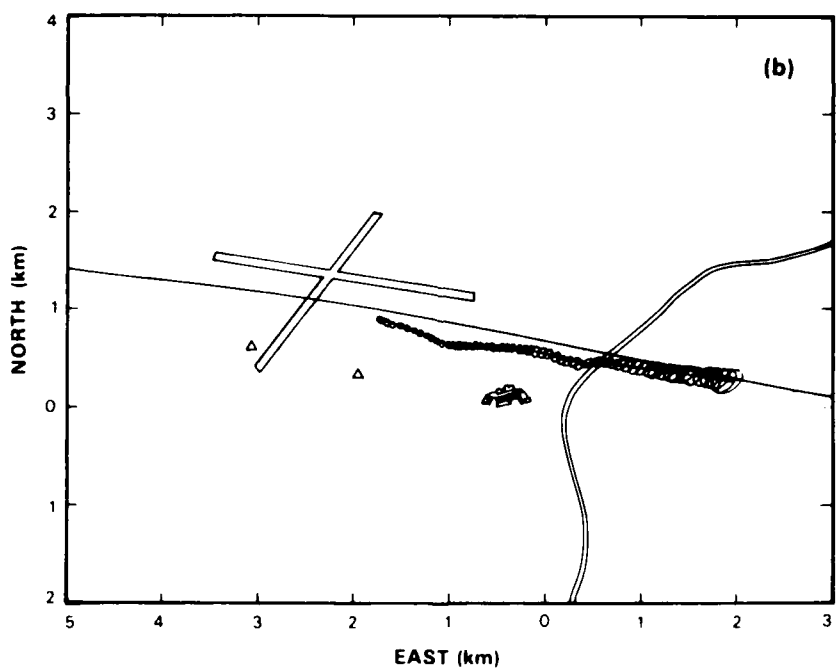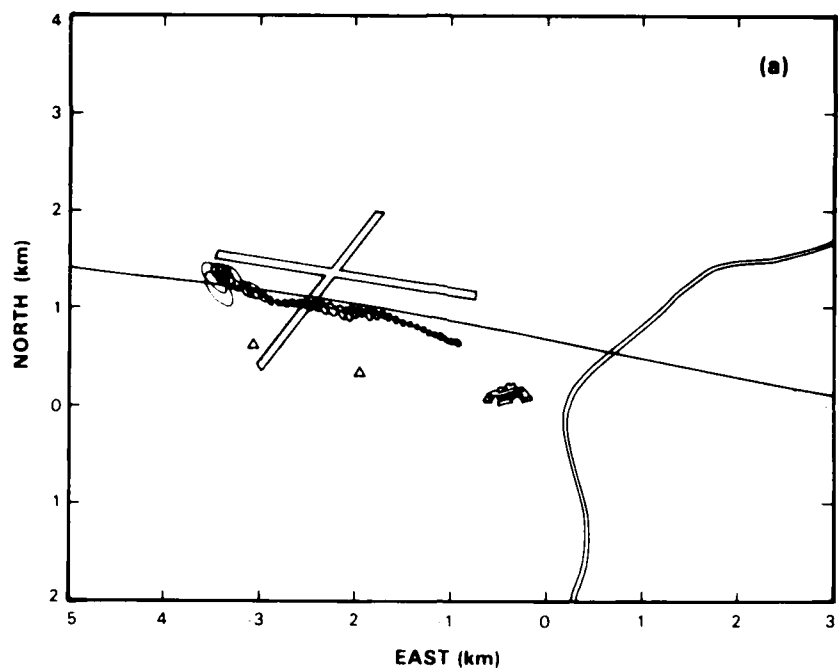
Figure IV-1. Helicopter tracking results for maximum communication policy: (a) Track produced by leftmost node; (b) track produced by rightmost node.

22

Figures IV-1 and IV-2 illustrate the results from one important pair of experimental runs. Figure IV-1 shows target tracks obtained for the case when position tracks were broadcast after each measurement. The nominal flight path is represented by a straight line. Outlines of the Hanscom Field runways, Lincoln Laboratory, and Route 128 are shown for scale. The locations of the four sensors that recorded the data are shown by triangles. For the case shown, all sensors were assumed to have a maximum detection range of 3 km and all nodes received broadcast directly from all other nodes. The tracks are shown by sequences of estimated error ellipses, with line segments connecting their centers which represent the estimated track. Figure IV-1(a) shows the track produced by the leftmost node, and IV-1(b) by the rightmost node.

The position track is first initiated through the cooperation of the two leftmost nodes. They actually detect the helicopter long before the track is initiated, but the nearly colinear geometry of the two nodes and the target prevent track initiation for almost a minute. The tracking error is reduced fairly rapidly and is quite small by the time the helicopter is abreast of the second sensor. At that time, the helicopter is just entering the nominal sensor coverage of the last node, and so its track begins. There is no transient tracking error because track initiation is not being repeated; the track is handed over. The first node drops its track a bit later when the helicopter is estimated to have passed out of its nominal coverage. The tracking is best for both nodes in the period of overlapping tracks because all four nodes are contributing measurement information during that period. The track quality degrades as the earlier nodes cease to detect the helicopter. Finally, even the last node ceases detecting it, roughly as it passes over Route 128. However, the track is maintained by coasting until the helicopter is estimated to have passed beyond the nominal 3-km detection range.

Figure IV-2 is equivalent except for one important change — the maximum time interval between broadcasts is set so large that only critical-event broadcasts occur. The track from the first node now has a much larger transient because it only has information from its own sensor between broadcasts. The track of the first node improves when the second node broadcasts to alert the third node that the helicopter is entering its coverage. But, only when the second and third nodes broadcast to alert the fourth is the track quality comparable to what it was much sooner for the situation of Figure IV-1. Note that the quality of the track initiated for the last node confirms that the information accumulated by the first three nodes, even with only a few broadcasts, is sufficient for good tracking.

B. TWO-NODE PERFORMANCE EVALUATION EXPERIMENTS

A number of two-node, one-target experiments have been performed to begin evaluating the sensitivity of acoustic tracking algorithms to three factors: (1) target velocity, (2) target trajectory, and (3) target maneuvers. The experiments were performed using two test-bed nodes, simulated single-target data corresponding to two acoustic sites separated by 5 km, and with tracker parameters set to the values used in the communication experiments reported in the previous section. These tracker parameters had been roughly adjusted to provide good performance for slow-speed nonmaneuvering targets without regard for what performance might be obtained for
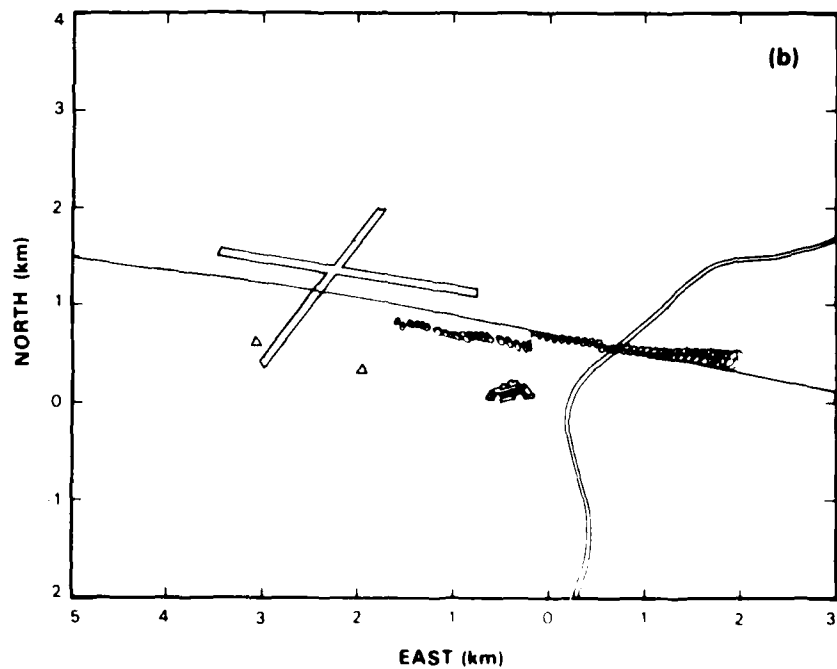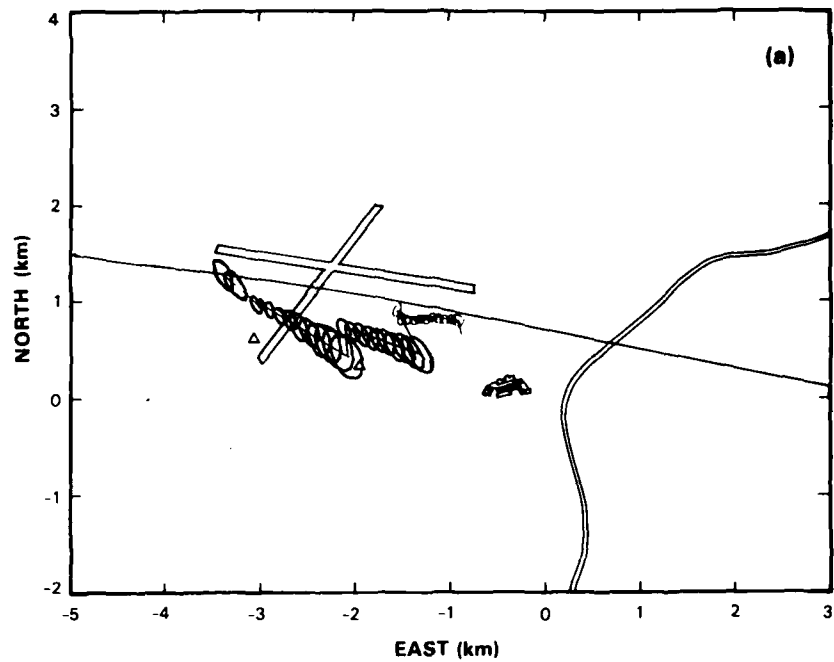
Figure IV-2.   Helicopter tracking results for minimal communication policy: (a) Track produced by leftmost node; (b) track produced by rightmost node.

24

other situations. The broadcast policy was to set the maximum time between broadcasts to be equal to the time between measurements: 2 s. This allowed us to investigate the characteristics of the tracking process without complications being introduced by the communication policy. The long-term objective of the experiments is to identify desired changes in the tracker parameters and enhancements which might be made in the tracker algorithm that can improve performance.

The data-collection procedure for each experiment is illustrated in Figure IV-3. Scenario and tracker parameters are specified for each experimental run. The scenario parameters describe the assumed target and sensor characteristics. The tracker parameters control the operation of the three parts of the tracking algorithm: (1) the measurement thresholding algorithm, which selects azimuth measurements on the basis of signal power or signal-to-noise ratio; (2) the azimuth tracking algorithm, which associates and combines measurements to initiate, continue, and terminate azimuth tracks; and (3) the position tracking algorithm, which associates and combines measurements to initiate, continue, and terminate position tracks. All outputs of these processes in each of the experimental nodes are saved for performance evaluation.
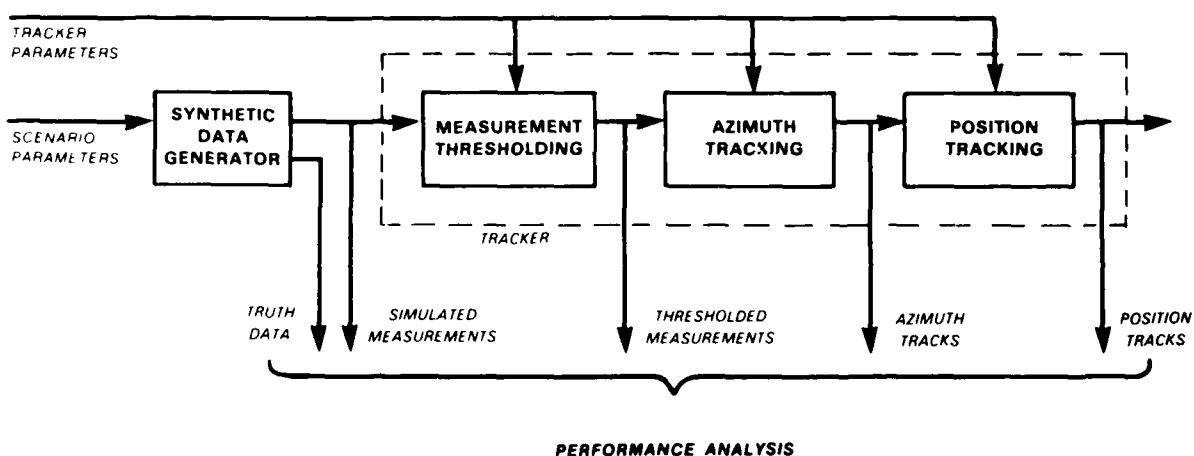
Figure IV-3.   Types of data collected for two-node tracker performance evaluation experiments.

Several quantitative performance measures are calculated from the tracker outputs. The performance measures for the three tracker outputs are: (1) range of the first and last detections for the measurement thresholding algorithm, (2) range corresponding to the first and last azimuth track points and the real and estimated azimuth errors along the azimuth tracks, and (3) the target range at the first and last track points and the real and estimated position errors for the position tracking algorithm.

The following summarizes results obtained to date from these sensitivity experiments. Figure IV-4 shows the six different target tracks that were used. They include straight-in and oblique tracks, tracks very close to one node as well as between the two nodes, and a dog-leg track.

25

Figure IV-4. Target trajectories used for performance evaluation experiments.
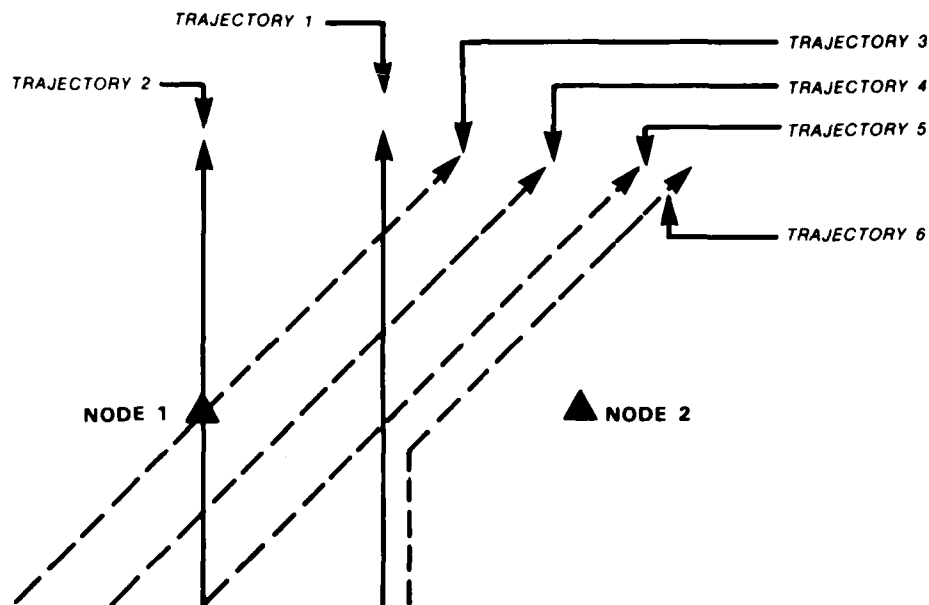
Velocity sensitivity experiments were run using track number 1 of Figure IV-4 and four different target velocities: Mach 0.1, 0.3, 0.6, and 0.8. These experiments showed significant velocity sensitivity for the tracking parameters that were employed.

Figure IV-5 shows examples of the azimuth tracks for Mach 0.1 and 0.6 velocity sensitivity experiments. Also shown are the ranges, R_1 and R_2, at which the target is first in azimuth track and at which azimuth track is lost. For the purpose of defining R_1 and R_2, the target is considered to be in track only if both the actual and estimated azimuth errors are less than $10°$. R_1 and R_2 are the distances from Node 1 to the sound source, not to the actual target location. The azimuth tracker performed better for the low-speed target, which is not surprising since the parameters were tuned for that case. For the Mach 0.3 case, the results were intermediate between the 0.1 and 0.6 cases; for the Mach 0.8 case, the azimuth tracks were somewhat poorer than for the Mach 0.6 case.

Two effects explain the azimuth tracking results shown in Figure IV-5. First, at faster velocities there are fewer azimuth measurements; measurements are made every 2 s in both cases. Several consecutive measurements are required to start an azimuth track so that the faster target is closer to the nodes by the time an azimuth track is initiated. This explains why R_1 is smaller for the faster target. Second, at faster velocities the angular acceleration of the target is larger. The azimuth tracker is based on a linear model with a random acceleration parameter which is suitable for slow, but not for fast, targets. Although there are other factors at play, this largely explains why the estimated track diverges from the true track in the case of the fast target.
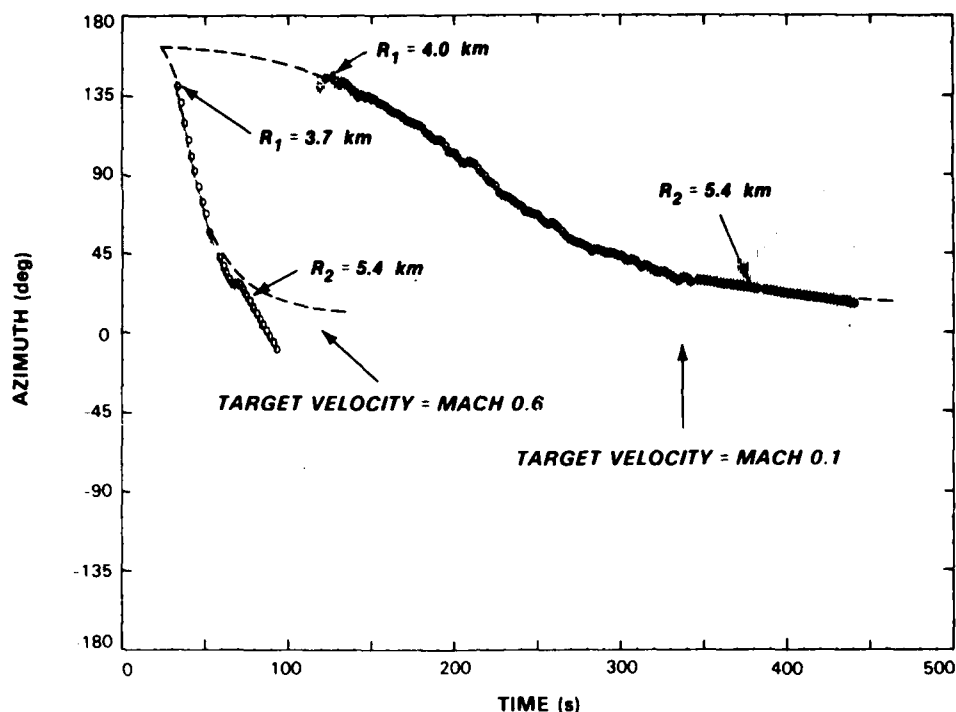
26

Figure IV-5. Effect of velocity on azimuth tracks.

Figure IV-6 shows position tracks for the same two runs shown in Figure IV-5. Also shown are the range (R_1) at which the tracks were initiated and the range (R_2) when the tracking error became greater than 1000 m. Tracks are initiated further along the true track and terminated sooner for the faster target. Furthermore, the true and estimated position errors are larger for the faster targets as shown in Figure IV-7 as a function of time. The estimated errors are the error estimates generated by the position tracking Kalman filter. For the Mach 0.6 case the estimated error is considerably less than the true error, indicating that the Kalman filter is mistuned for higher velocities.

Tracking performance at Mach 0.3 was intermediate between the Mach 0.1 and 0.6 cases. The tracker did not initiate any position tracks for the Mach 0.8 case.

A second series of experimental runs was made to investigate the effect of oblique target approaches and approaches that pass very near one of the nodes. Target velocity was held constant at Mach 0.1 in all cases. These experiments showed that the performance of the present algorithms deteriorates when the target flies over or near one of the nodes or the approach to the node pair is oblique.
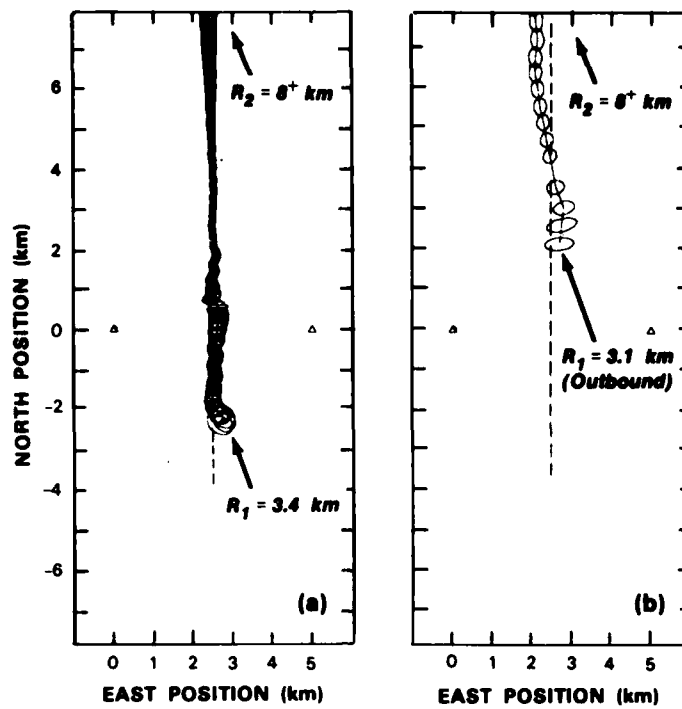
27

Figure IV-6.   Effect of velocity on position tracks: (a) Track for Mach 0.1 target; (b) track for Mach 0.6 target.
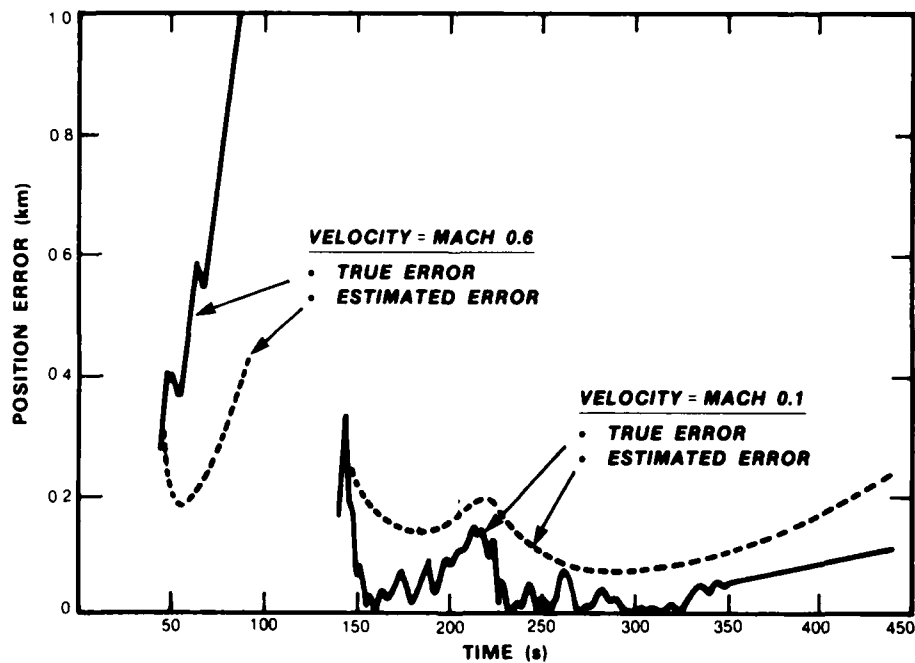

Figure IV-7.   Estimated and measured positions errors for Mach 0.1 and 0.6 targets.

28

When a target flies directly over a node, the azimuth tracker failure mode is such that the azimuth track is lost and a new track is initiated as the azimuth suddenly switches by 180°. Even with this azimuth tracking problem, the position tracker should generate a position track if azimuth measurements from a second node are available. Unfortunately, we discovered that the measurement thresholding parameters used for these experiments did not provide a second track when the target was 5 km away, as it does for a direct overflight of one of the nodes. Additional runs are being planned with different thresholding parameters.

The oblique trajectories (Trajectories 3 to 5 in Figure IV-4) affect performance in two ways: (1) the track is initiated later than in the symmetric trajectory case, and (2) larger position errors are obtained. These effects, which are a result of the target/node geometry, are more pronounced when the target crosses the baseline closer to one of the nodes.

The sensitivity to two kinds of target maneuvers has been investigated: (1) a change-of-velocity maneuver, and (2) a change-of-trajectory ("dog-leg") maneuver. For the change-of-velocity experiment, the target followed Trajectory 1 in Figure IV-4, changing velocity from Mach 0.1 to 0.2 upon crossing the baseline connecting the nodes. For the dog-leg maneuver experiment, the target followed Trajectory 6 in Figure IV-4, changing from a 0° to a 45° course upon crossing the baseline.

Figure IV-8 shows the position track for the experiment in which the target changes velocity from Mach 0.1 to 0.2 upon crossing the baseline between the nodes. Figure IV-9 shows the actual
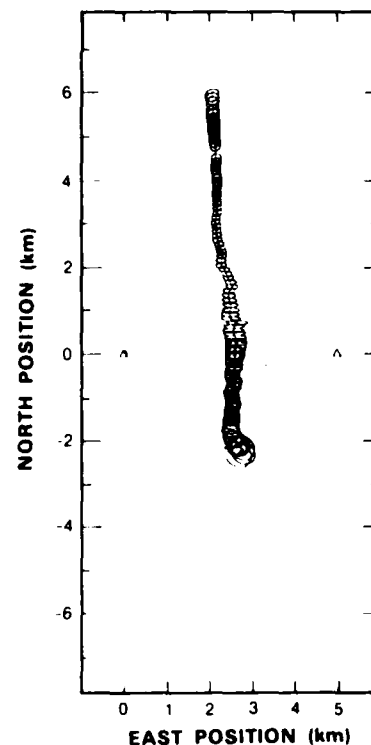
Figure IV-8. Target track for a velocity change from Mach 0.1 to 0.2 at a point between the two tracking nodes.
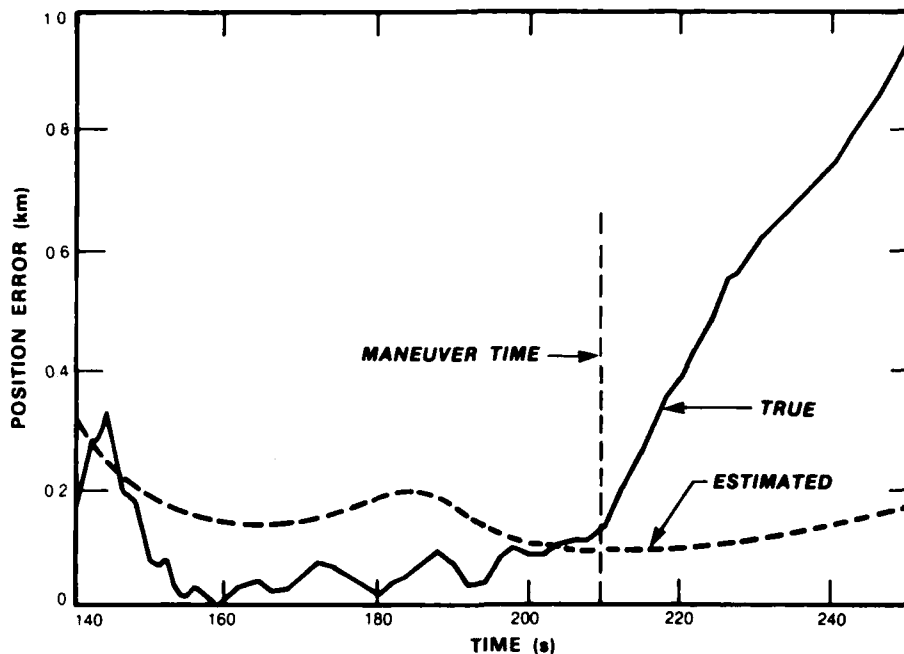

29

*Figure IV-9. Tracking errors for change-of-velocity maneuver.*

path errors as a function of time. The true error begins to grow at the time of the maneuver. The estimated error, however, remains small showing that the filter is not tuned to respond to such maneuvers. Most of the increasing error is along the direction of the trajectory, which is to be expected.

Figure IV-10 shows the position track for the dog-leg maneuver experiment, and Figure IV-11 shows the true and estimated errors as a function of time. As in the case of the change-of-velocity maneuver, the position error begins to increase when the maneuver is performed, but the error estimated by the Kalman filter remains small. Unlike the change-of-velocity maneuver, the filter does recover somewhat before the target leaves the detection range of the nodes. Of course, in a DSN with many nodes, other nodes would contribute to the tracks and recovery would eventually be complete in all cases.

In summary, these experiments have identified a number of sensitivities in tracking performance which are present for two-node configurations and will also be present, but perhaps less significant, when more than two nodes are involved. Mechanisms have been identified for these sensitivities, and information has been gained to assist in further tuning of the tracker parameters to handle a wider range of situations.

30

Figure IV-10.   Two-node position track for dog-leg maneuver.
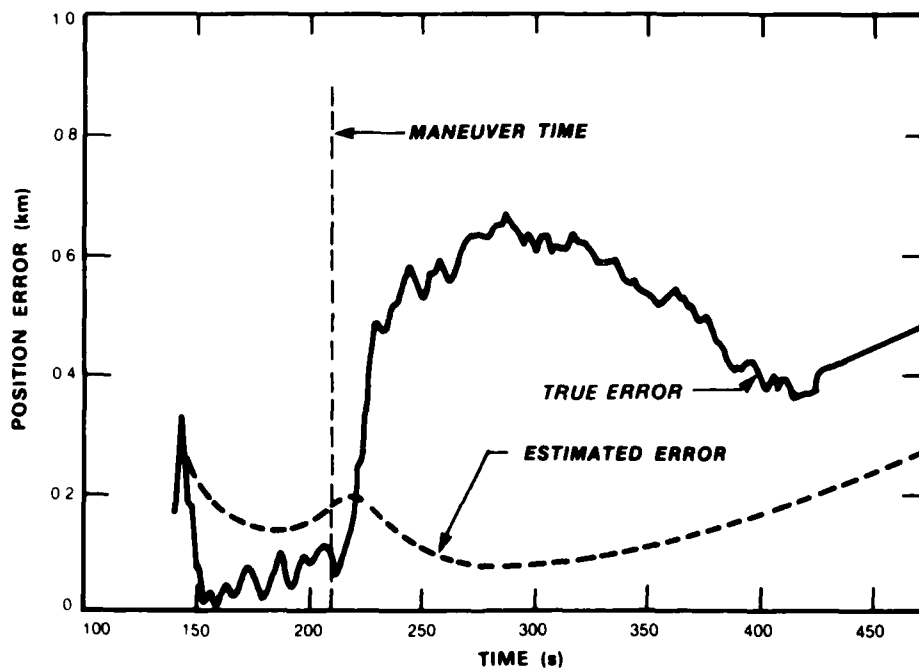True track is shown dashed.
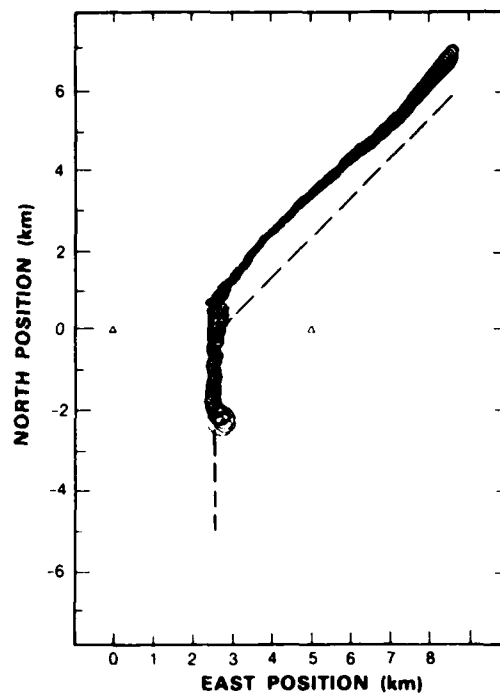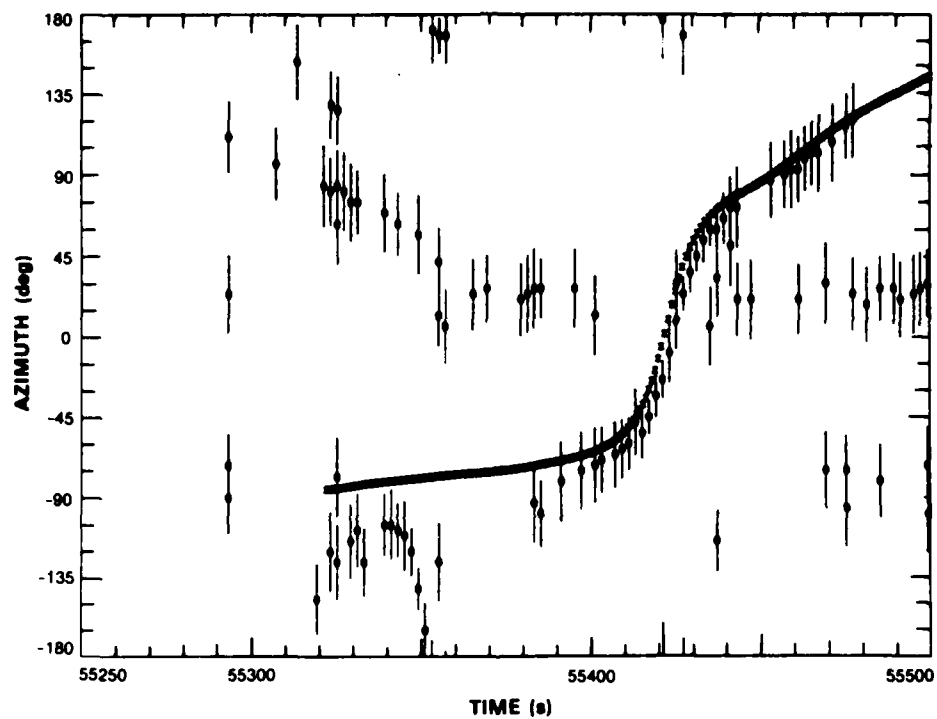
Figure IV-11.   Tracking errors for dog-leg maneuver.

31

Figure IV-12. Acoustic azimuth measurements and ground-truth data for instrumented Cessna 402 aircraft.

C. CESSNA 402 DATA COLLECTION AND ANALYSIS

During this reporting period, the opportunity arose to perform some exploratory experiments with a model 402 Cessna with on-board instrumentation to precisely record the position of the aircraft (ground truth) based upon distance measuring and inertial navigation equipment. These experiments have a number of uses, a major one being to prepare for future experiments with another aircraft that will be similarly instrumented and will be available for more extensive experimentation. The Cessna experiments also provided a test of a new array which was installed in the woods near the Laboratory. The new data will also be used for further experimentation with signal processing and tracking parameters. In addition, the quietness of the aircraft presented an interesting problem in low-level signal detection in a noisy environment, and allowed us to experiment with noise-reducing barriers to reduce specific fixed-noise sources.

Acoustic data were collected on several occasions. In the initial tests, we found that the new array in the woods had by far the best signal-to-noise ratio, although it was the farthest from the flight path. This was due to the low environmental noise level at the new site. The two older installations are on rooftops and are close to stationary noise sources such as ventilation fans. In addition to being loud, the fans produce noise tones at a frequency very close to the fundamental frequency from the Cessna aircraft propeller, which is the major sound source for this aircraft. After the initial tests showed this, we installed an acoustic baffle between one of the arrays and a nearby ventilator, and the signal-to-noise ratio for this array improved markedly. A similar barrier is now being installed at the other array.

The Cessna data are quite different from previously analyzed helicopter or jet-aircraft data. Some experimentation has been done with the signal processing parameters to improve the quality of azimuth peaks obtained. In particular, we found it useful to utilize a wider prefiltering frequency band than that used for helicopters and jets. This wider band included both the fundamental frequency of the propeller and its second harmonic for detection and estimation of azimuths. We also found the application of a windowing function to the data to be helpful. An example of the azimuth measurements obtained may be found in Figure IV-12 which shows data collected from the new array in the woods. The detections from the signal processing and measurement process are shown as small circles with vertical error bars attached. The solid line is the true acoustic azimuth vs time for the target as calculated from the ground-truth records made on-board the aircraft. Further analysis of these data and experimentation with tracking parameters are under way at the present time.

33

V. KNOWLEDGE-BASED SYSTEM DIAGNOSIS

During this report period, the implementation of an experimental signal processing diagnosis system was completed as well as key portions of a system which decides how to change DSN parameters in response to the diagnosis. These systems demonstrate the feasibility of using current Artificial Intelligence technology for automated diagnosis of a complex algorithmic system such as the DSN signal processing system.

The diagnosis system takes as inputs hypothetical signal processing results for situations which involved either incorrectly set DSN parameters (e.g., filter passbands do not overlap with aircraft frequencies) or aircraft 'scenarios for which the DSN system has limited capabilities (e.g., two aircraft with bearings that are too close for the limited aperture of the DSN array). The output of the diagnosis system is in the form of diagrams that describe how particular DSN processes led to the characteristics observed in the signal processing outputs. Figure V-1 is an example of a diagnosis provided by the system. In this case, the system has decided that a combination of directional uncertainty for a high-speed aircraft and limited array aperture has resulted in the detection of a false bearing. The "fast-velocity operator" and the "equal-resolution operator" mentioned in the diagnosis are illustrated in Figures V-2 and V-3. These descriptions specify the preconditions that must hold for these operators to apply, as well as postconditions that describe the consequence of operator application. These conditions are specified at different levels of abstraction because our system can handle different degrees of certainty in the information regarding the actual aircraft scenario.
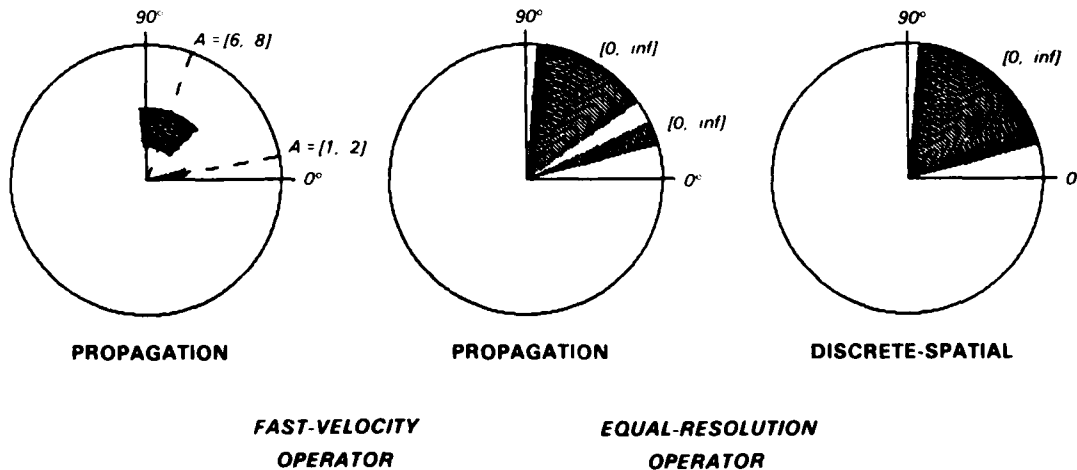

157966-N

Figure V-1. Diagnosis display produced by knowledge-based signal processing diagnosis system.

35

INPUT SIGNAL TYPE	propagation
OUTPUT SIGNAL TYPE	propagation
DIFFERENCES REDUCED	direction-shift, amplitude-scaling
OPERATOR PARAMETERS	
DIRECTION	analysis-interval > 0.5
POWER	analysis-interval > 0.5
FREQUENCY	analysis-interval > 0.5
BAND	analysis-interval > 0.5
GAUSSIAN	analysis-interval > 0.5
STATE PRECONDITIONS	per input signal
DIRECTION	Direction in [0, 360].
POWER	Direction level preconditions.
	Power in [0, inf].
FREQUENCY	Direction level preconditions.
	Minimum-freq in [0, maximum-freq].
	Maximum-freq in [0, inf].
BAND	Power level preconditions.
	Frequency level preconditions.
	Amplitude in [0, inf].
GAUSSIAN	Band level preconditions with Gaussian model.
SCENARIO PRECONDITIONS	per individual aircraft
	Distance < 5 km.
	Velocity > (200/analysis-interval) m/s.
POST CONDITIONS	changes per input signal
DIRECTION	Direction shift by 3*analysis-interval.
POWER	Direction level postconditions.
	Power scaled by 1/(3*analysis-interval).
FREQUENCY	Direction level postconditions.
BAND	Power level postconditions.
	Frequency level postconditions
	Amp scaled by 1/(3*analysis-interval).
GAUSSIAN	Band level postconditions with Gaussian model.

Figure V-2. "Fast-velocity" operator used by diagnosis system.

157967-N

36

INPUT SIGNAL TYPE	propagation, continuous-temporal, discrete-temporal, continuous-spatial
OUTPUT SIGNAL TYPE	continuous-spatial
DIFFERENCES REDUCED	resolution
OPERATOR PARAMETERS	
DIRECTION	array-aperture
POWER	array-aperture
FREQUENCY	array-aperture, epsilon
BAND	array-aperture, epsilon
GAUSSIAN	array-aperture, epsilon
STATE PRECONDITIONS	per pair of input signals
DIRECTION	Direction difference intersects [0, 100/array-aperture].
POWER	Direction level preconditions. Power in [0, inf].
FREQUENCY	Minimum-freq's intersect. Maximum-freq's intersect. Direction difference intersects [0, 1000*epsilon)/(array-aperture*.0001*maximum-freq].
BAND	Power level preconditions. Frequency level preconditions. Amp in [0, inf].
GAUSSIAN	Frequency level preconditions with Gaussian model.
SCENARIO PRECONDITIONS	none
STATE POSTCONDITIONS	per pair of input signals
DIRECTION	Delete input signals. Create signal whose direction is the cover of the two input directions.
POWER	Direction level postconditions. Power of output signal in [0, sum of maximum powers in signals].
FREQUENCY	Direction level postconditions. Minimum-freq of output same as input. Maximum-freq of output same as input.
BAND	Frequency level postconditions. Power level postconditions. Amp of output signal in [0, sum of maximum amps in signals].
GAUSSIAN	Band level postconditions with Gaussian model.

Figure V-3. "Equal-resolution" operator used by diagnosis system.

157968-N

The qualitative reasoning system to prescribe changes in DSN parameters for overcoming the problems identified in the diagnosis is also being implemented on a Lisp machine. This system utilizes qualitative models* of how the actions of operators are affected by parameter changes. We have implemented and tested such models for some of the DSN operators. This work was facilitated by the use of the QSIM[†] software package developed at M.I.T. for qualitative reasoning applications. However, we had to make a number of changes to account for the particular features of our DSN application.

---

* B.J. Kuipers, "Common-Sense Reasoning About Causality: Deriving Behavior from Structure," Artificial Intelligence **24** (1984).

† C. Eliot, QSIM Installation Notes, Clinical Decision Making Group, Laboratory for Computer Science, M.I.T. (1984).

GLOSSARY

DSN	Distributed Sensor Networks
NRTS	Nodal Run-Time System
QSIM	Qualitative Simulation
SATS	Semiannual Technical Summary
SGI	Silicon Graphics, Inc.
SNC	Standard Nodal Computer
SPS	Sound Processing Subsystem
UIP	User Interface Program

SECURITY CLASSIFICATION OF THIS PAGE *(When Data Entered)*

REPORT DOCUMENTATION PAGE		READ INSTRUCTIONS BEFORE COMPLETING FORM
1. REPORT NUMBER ESD-TR-85-287	**2. GOVT ACCESSION NO.** AD-A163 866	**3. RECIPIENT'S CATALOG NUMBER**
4. TITLE *(and Subtitle)* Distributed Sensor Networks		**5. TYPE OF REPORT & PERIOD COVERED** Semiannual Technical Summary 1 April — 30 September 1985
		6. PERFORMING ORG. REPORT NUMBER
7. AUTHOR(s) Richard T. Lacoss		**8. CONTRACT OR GRANT NUMBER(s)** F19628-85-C-0002
9. PERFORMING ORGANIZATION NAME AND ADDRESS Lincoln Laboratory, MIT P.O. Box 73 Lexington, MA 02173-0073		**10. PROGRAM ELEMENT, PROJECT, TASK AREA & WORK UNIT NUMBERS** Program Element No. 62708E Project Nos. 5D30 & 5T10 ARPA Order 3345
11. CONTROLLING OFFICE NAME AND ADDRESS Defense Advanced Research Projects Agency 1400 Wilson Boulevard Arlington, VA 22209		**12. REPORT DATE** 30 September 1985
		13. NUMBER OF PAGES 50
14. MONITORING AGENCY NAME & ADDRESS *(if different from Controlling Office)* Electronic Systems Division Hanscom AFB, MA 01731		**15. SECURITY CLASS.** *(of this Report)* Unclassified
		15a. DECLASSIFICATION DOWNGRADING SCHEDULE

16. DISTRIBUTION STATEMENT *(of this Report)*

Approved for public release; distribution unlimited.

17. DISTRIBUTION STATEMENT *(of the abstract entered in Block 20, if different from Report)*

18. SUPPLEMENTARY NOTES

None

19. KEY WORDS *(Continue on reverse side if necessary and identify by block number)*

multiple-sensor surveillance system	acoustic sensors	digital radio
distributed tracking	video sensors	distributed estimation
target surveillance and tracking	low-flying aircraft	knowledge-based data interpretation
communication network	acoustic array processing	

20. ABSTRACT *(Continue on reverse side if necessary and identify by block number)*

This report describes the work performed on the DARPA Distributed Sensor Networks Program at Lincoln Laboratory during the period 1 April through 30 September 1985.

DD FORM 1473 **EDITION OF 1 NOV 65 IS OBSOLETE**
1 Jan 73

SECURITY CLASSIFICATION OF THIS PAGE *(When Data Entered)*